EFFECT OF AGING CONCRETE ON SEISMIC PERFORMANCE OF SHEAR WALL STRUCTURES

L. Ibarra,[1] B. Dasgupta,[2] and K. Chiang[2]
[1]University of Utah, Department of Civil Engineering, Salt Lake City, Utah, USA
[2]Center for Nuclear Waste Regulatory Analyses, Southwest Research Institute®, San Antonio, Texas, USA
E-mail of corresponding author: bdasgupta@swri.org

ABSTRACT

This study evaluates the effect of concrete aging on the probabilistic seismic performance of structures that include shear walls as the main lateral resistance component. The scope of this work encompasses (i) identification of aging mechanisms of concrete and their effect on mechanical properties of reinforced concrete (RC) components; (ii) development of an approach to predict system capacity and generation of fragility curves that account for concrete aging; and (iii) evaluation of the effect of RC aging on the probability of failure under seismic events. Evaluations of seismic performance of nuclear facilities are based on seismic probabilistic risk analyses that do not include the effects of concrete aging. The seismic performance of safety-related structures may decrease because concrete properties degrade with time. Several studies have shown that the number of incidents related to concrete aging increases as the facilities age.

This study relates the physical mechanisms that take place during aging of concrete (e.g., cracking, rebar corrosion, and spallation) and the deterioration of mechanical properties that affect the system capacity under seismic events. The seismic performance evaluation uses available experimental data on the corrosion of steel reinforcement and variability of concrete parameters as a function of time. The evaluated concrete aging mechanisms are being correlated to the mechanical properties of the material. To obtain the variation in the system capacity caused by concrete aging, detailed numerical models of reinforced concrete components and models of the selected structural systems are being developed.

The probability of unacceptable performance or seismic failure is computed by convolving the fragility and selected hazard curves. Failure probability increases with aging of RC, the increase on the concrete compressive strength with time, however, does not overcome the degradation of seismic performance caused by concrete cracking and corrosion of steel rebars. The results indicate that aging effects on RC also depend on the seismic hazard at the site. Aging effects increase the probability of failure of RC reinforced concrete shear walls subjected to lateral loading, but the increase is less than one order of magnitude when all sources of variability are considered.

INTRODUCTION

The seismic performance of RC structures may be adversely affected by aging of concrete, which modifies the material engineering properties and affects the dynamic properties, structural resistance capacity, failure modes, and location of failure initiation. The degradation of reinforced concrete structures due to aging of concrete can be caused by (i) adverse performance of either the cement matrix or aggregate materials under an aggressive chemical environment; (ii) physical challenges including thermal cycling, abrasion, and vibration; and (iii) corrosion of steel reinforcing bars (rebars), which leads to cracking and spalling of the concrete cover. In general, RC structural components have substantial safety margins when properly designed and constructed, but the safety margins for aged concrete structures are not well understood. Therefore, a reliability-based methodology is being developed to assess the seismic performance of shear wall structures subjected to the aging of concrete. Nuclear facilities commonly use shear walls to withstand lateral loads, and during license renewal, a safety and risk assessment that accounts for aging deterioration of reinforced concrete components may be needed. Evaluations of seismic performance of nuclear facilities are based on seismic probabilistic risk analysis [1] that does not include the effects of concrete aging, which may increase the potential for failure. Several studies have shown that the number of incidents related to concrete aging increases as the facilities age. Braverman, et al. [2] concluded that concrete aging needs to be considered in a structural performance assessment.

This study evaluates the effect of concrete aging on the probabilistic seismic performance of structures that include shear walls as the main lateral resistance component. The scope of this work encompasses (i) identification of aging mechanisms of concrete and their effect on mechanical properties of reinforced concrete (RC) components;

(ii) development of an approach to predict system capacity and generation of fragility curves that account for concrete aging; and (iii) evaluation of the effect of RC aging on the probability of failure under seismic events.

This investigation relates the physical mechanisms that take place during aging of concrete (e.g., cracking, rebar corrosion, and spallation) and the deterioration of mechanical properties that affect the computation of the system capacity under seismic events. The study includes available experimental data about steel corrosion and variation of concrete compressive strength as a function of time. To obtain the variation in the system capacity caused by concrete aging, finite element models (FEMs) of RC components were developed. Several studies have modeled structural components to represent aging of concrete [2,3], but the effects on RC components usually are not extrapolated to the entire structural system. The ultimate goal of this research is to evaluate aging effects on the behavior of a typical multi-storied nuclear facility structural system consisting of shear walls, diaphragm slabs, and basemat.

The variability in the response due to uncertainty in the system parameters was obtained using a Latin Hypercube Sampling approach. The probability of unacceptable performance or seismic failure was computed by convolving the fragility and hazard curve.

Calibration of Shear Wall Components in Numerical FEMs

Structural systems with shear wall components were created in SAP2000 [4] to evaluate the effects of aging concrete on system structural performance. Shear wall components were created to calibrate the FEM and to identify the main parameters that control the effect of aging on seismic performance. A flanged shear wall was modeled to reproduce the second specimen tested by Barda et al. [5] under monotonic lateral loading (Fig. 1a). The central shear wall has a length l_w = 191 cm (75 in), height h_w = 95.3 cm (37.5 in) (i.e., aspect ratio l_w/h_w = 0.5), and thickness t_n = 10.2 cm (4 in). Because of the low aspect ratio, the component is expected to exhibit shear failure. The mesh was created using the shell-layered non-linear element of SAP2000, which can reproduce the nonlinear response of confined and unconfined concrete. For the nonlinear performance of concrete, the stress-strain constitutive relationship was based on Mander's model [6]. As seen in Fig. 1b this model captures the softening of the stress-strain curve for confined and unconfined behavior of concrete, and the shear wall response can be predicted after some of the shell elements have reached the ultimate strength.

The FEM was able to reproduce the expected in-plane shear stresses obtained by Barda et al. [5]. The base shear at ultimate strength of the component is presented in the pushover curve as shown in Fig. 2. This curve represents the static nonlinear relationship between the top of the central shear wall and the applied lateral load. The mean base shear at ultimate strength obtained from SAP2000 analysis was 930 kN (209 kips) as shown in Fig. 3, which is within 5% of Barda's experimental test (978 kN (220 kips)) [5]. The displacement at the ultimate strain, however, was lower than the displacement obtained from the experiment where the flanges exhibited nonlinear behavior. The results from this model and additional shear wall models with no flanges, however, demonstrated that the shell-layered nonlinear element is capable of reproducing the in-plane response of reinforced concrete shear walls.

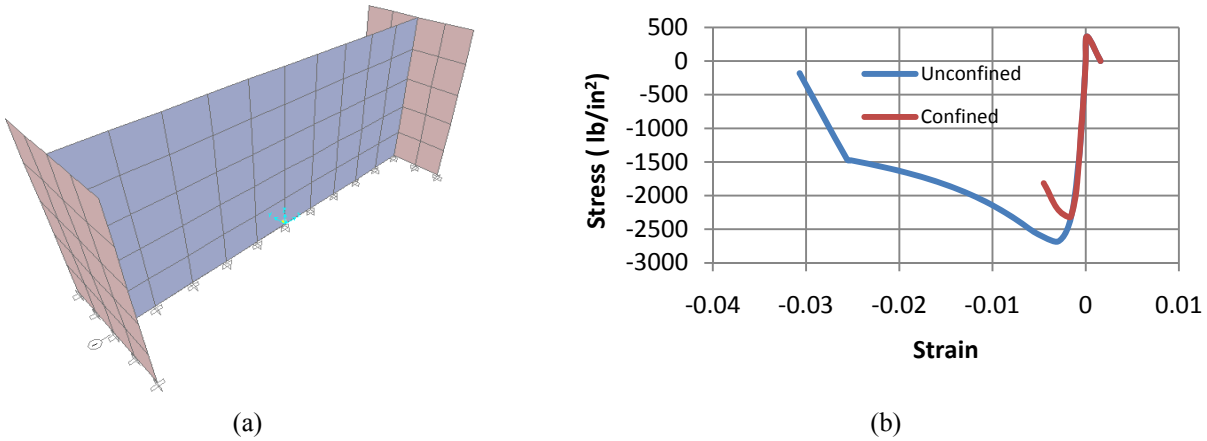

(a) (b)

Fig. 1. (a) Tridimensional View of the Shear Wall With Flanges Used for Numerical Simulation, (b) Mander's Stress-Strain Model for Unconfined and Confined Concrete Model.

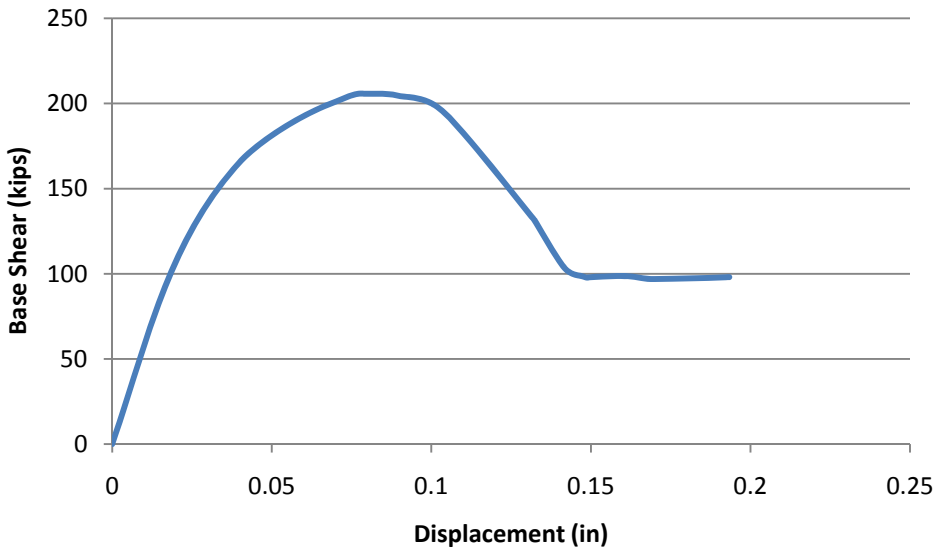

Fig. 2. Pushover Curve Displacement Versus Base Reaction for Calibrated Shear Wall Model.

Numerical Simulation of a Shear Wall Component

After the behavior of low-aspect ratio shear walls was verified in the FEM, a rectangular (no flange) shear wall component was modeled as lateral resistance system. The effect of variability of degraded and non-degraded parameters for the limit states of interest was investigated to assess the ultimate strength of the shear wall. The limit state is approximated in models as the strength corresponding to an inter-story drift of 0.4 percent [7]. The evaluated shear wall model has a length l_w = 7.3 m (24 ft), height h_w = 3.65 m (12 ft) (i.e., aspect ratio l_w/h_w = 0.5), and thickness t_n = 0.3048 m (1 ft).

The design concrete compressive strength (f_c') was 27.6 MPa (4,000 psi). However, the information obtained from cylinder tests and concrete cores [8] was used to define f_c' for degraded and non-degraded components. The concrete compressive strength, f_c' at 28 days was 33.1 MPa (4,800 psi) and f_c' = 41.6 MPa (6,030 psi) for concrete older than 5-10 years. The vertical reinforcement steel consisted of rebar No. 6 (i.e., diameter of 19mm (¾ in)) spaced at each 0.304 m (12 in).

To correlate the lateral force ($F_{lateral}$) applied to the shear wall to seismic load, it is assumed the lateral force is caused by a rigid reinforced concrete slab that transfers a total weight (W) of 2224 kN (500 kips). Thus the force is related to the spectral acceleration, S_a, as

$$F_{lateral} = m.S_a = WS_a/g \quad \text{(Eq. 1)}$$

where, g is the acceleration due to gravity.

Fragility for Non-degraded Shear Wall Component

To obtain the variability in the response for non-degraded elements, the probabilistic distribution initially proposed by Braverman et al. [2] for random parameters were used (Table 1).

The variance on the ultimate strength of the component due to variability of the previously described input parameters can be obtained using Monte Carlo simulation. The approach is efficient to obtain the variability in the response, but it is time consuming because thousands of realizations are required and each finite element simulation takes longer time. To circumvent this shortcoming, a Latin Hypercube Sampling (LHS) approach was implemented [9]. The LHS approach significantly reduces the number of finite element realizations because values for the different probabilistic parameters are based on non-overlapping intervals with equal probability. Following this approach and using the data from Table 1, the input probabilistic parameters of Table 2 were computed for 20 realizations.

The input parameter values from the 20 realizations were used to obtain the structural response of the shear wall model. The push-over curves for all the realizations are shown in Fig. 3. The mean value of lateral force at the ultimate strength is 9208 kN (2,070 kips), which is equivalent to a spectral acceleration S_a = 4.14 g (from Eq. 1). The standard deviation is

Table 1. Probabilistic Parameters for Non-Degraded Reinforced Concrete Shear Walls
(1 psi = 0.006894 MPa)

Parameter	Mean	Coefficient of Variation	Distribution
Concrete compressive strength, f_c'	4,000 psi	0.16	Normal
Concrete modulus, E	$57{,}000\sqrt{f_c'}$ psi	0.18	Normal
Strain at ultimate strength, ε_c	0.004	0.20	Normal
Steel yield strength, f_y	66,000 psi	0.10	Lognormal

Table 2. Realizations for the Input Probabilistic Parameters of the Shear Wall
(1 psi = 0.006894 MPa)

	f_c' (psi)	E (psi)	ε_c	f_y (psi)	f_u (psi)
1	4,827	4,529,880	0.00548	64,646	96,968
2	5,910	5,723,103	0.00584	65,901	98,851
3	4,389	2,800,119	0.00411	69,719	104,579
4	4,983	4,716,957	0.00479	75,515	113,272
5	4,276	3,050,165	0.00520	59,701	89,552
6	6,560	4,231,703	0.00647	67,036	100,555
7	4,633	3,760,032	0.00359	57,647	86,471
8	4,057	3,723,239	0.00223	72,726	109,089
9	5,762	4,697,855	0.00510	61,013	91,519
10	4,453	5,779,559	0.00589	62,441	93,662
11	5,163	5,680,761	0.00446	54,997	82,495
12	2,888	2,918,562	0.00527	63,568	95,351
13	5,001	3,886,603	0.00683	64,320	96,480
14	4,529	5,370,754	0.00488	73,308	109,961
15	5,407	3,478,962	0.00616	67,934	101,901
16	5,536	5,264,678	0.00467	70,932	106,399
17	3,565	3,105,226	0.00559	66,283	99,425
18	3,860	3,450,382	0.00427	60,198	90,297
19	4,759	4,048,249	0.00394	68,865	103,297
20	5,298	3,988,828	0.00453	77,499	116,249

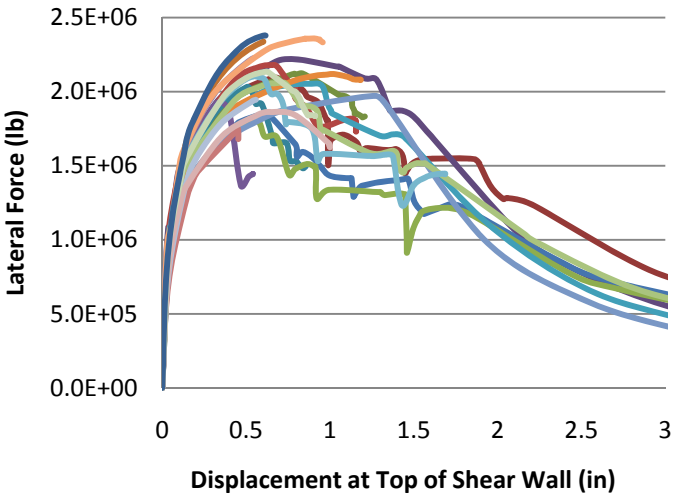

Fig. 3. Pushover Curves for the Lateral Force—Top Shear Wall Displacement. Non-degraded Reinforced Concrete Shear Wall.

818 kN (184 kips) (S_a = 0.37 g), resulting in a rather small coefficient of variation of 0.09. As expected, the mean S_a for the 20 realizations is very close to the spectral acceleration of the baseline case (S_a = 4.18 g). The base shear, V_u, was also obtained using the ASCE/SEI 43-05 [2,5] equation without a capacity reduction factor:

$$V_u = t_n d \left(8.3\sqrt{f_c'} - 3.4\sqrt{f_c'}\left(\frac{h_w}{l_w} - 0.5\right) + \frac{N}{4 l_w t_n} + \rho_{se} f_y\right) \quad \text{(Eq. 2)}$$

where N is the axial load, the effective wall depth is $d = 0.6 l_w$, and ρ_{se} is the equivalent steel reinforcement, which for walls with $l_w/h_w \leq 0.5$ is equivalent to the vertical steel reinforcement ratio ρ_v [7]. The base shear at ultimate strength obtained from Eq. 2 is 9030 kN (2,030 kips), which is only 3 percent less than the capacity derived from the nonlinear FEM. This shows that the empirical wall depth equivalent to 60 percent of the wall length, l_w, is a good approximation to obtain the ultimate shear strength. Note that a large part of the variability in the response when using the ASCE/SEI 43-05 [7] equation is caused by the uncertainty in the wall depth.

Regarding the interstory drift, ASCE/SEI 43-05 [7] recommends a limit of 0.4 percent, which for a wall with h_w of 3.7 m (12 ft) results in a drift limit of 14.6 mm (0.576 in). As observed in Fig. 3, this limit is acceptable for most cases, although a couple of realizations reached the ultimate strength at drifts less than 0.4 percent. Moreover, in most realizations the components experience significant nonlinear behavior, and consequently permanent damage, at drifts that are significantly lower than the previously described threshold.

Fragility for Degraded Shear Wall Component

To obtain the fragility curve for the degraded case, aging effects were considered for several input system parameters. Note that, unlike the rest of the parameters, the concrete compressive strength increases as the structure ages, as well as the concrete modulus that is related to f_c'. For this example, the mean f_c' value was increased from 33.1 MPa (4,800 psi) at 28 days to 41.6 MPa (6,030 psi) for long-term evaluation and the coefficient of variation was increased from 0.16 to 0.18 to account for increase in uncertainty in aging of concrete. The concrete modulus was increased accordingly. The strain at the ultimate strength, ε_c, was assumed to degrade with time to account for potential brittleness of aging concrete. Also, the softening slope of the stress-strain curve for the confined concrete material was increased from $-0.10E_c$ for non-degraded case to $-0.15E_c$ for the degraded case. The steel area was reduced by an average of 20 percent to account for steel corossion caused by crack widths of about 0.9 mm (0.354 in) [2]. Finally, the softening slope of the stress-strain curve of steel material was increased from $-0.10E_s$ for non-degraded case to $-0.15E_s$ for degraded case Table 3 summarizes these modifications.

Table 3. Probabilistic Parameters for Degraded Reinforced Concrete Shear Walls (1 psi = 0.006894 MPa)

Parameter	Mean	Coefficient of Variation	Distribution
Concrete compressive strength, $f_c^{'}$	6,800 psi	0.18	Normal
Concrete modulus, E	$57{,}000\sqrt{f_c^{'}}$ psi	0.18	Normal
Concrete strain at ultimate strength, $\varepsilon_{c,deg}$	$0.80\varepsilon_c$	0.10	Normal
Softening slope concrete stress-strain	$-0.15E_c$	0.15	Normal
Steel area reduction, $A_{s,red}$	$0.80A_s$	0.15	Lognormal
Softening slope steel stress-strain	$-0.15E_s$	0.15	Normal

Fig. 4a shows the fragility curve obtained from 20 realizations for the degraded and non-degraded systems. Log normal distribution was assumed for the fragility curve [2,10] and the mean and standard deviation were obtained from the results of the base shear at the ultimate strength for the 20 realizations. The cases with very low base shear at ultimate strength correspond to wall with loss of steel area was significant. The mean base shear at ultimate strength decreased about 14 percent for the degraded case, and the standard deviation of the data increased from 0.09 to 0.17. The increase in the dispersion is reflected in the flatter slope of fragility curve for the degraded case. The results show that an increase in the compressive strength of concrete with time is not sufficient to overcome the aging effects caused by the rest of the degraded parameters (e.g. concrete cracking and corrosion of steel).

Although the variability in the response considers linear and nonlinear input parameters (capacity parameters), it does not account for variability in the frequency content of ground accelerations [also called record-to-record (RTR) variability]. Previous studies have shown [10] that the variability of short period systems caused by RTR variability corresponds to a coefficient of variation (c.o.v.) in the range of 0.20 to 0.35. To assess aging effects, the variability in the demand and capacity parameters must be considered. Thus, for this study the variability in the response due to RTR variability (demand parameters) was included by assuming a c.o.v. = 0.25. The total variance in the response (σ_{tot}^2) can be assumed as the sum of the variance due to uncertainty in the system parameters (σ_{sys}^2) and the variance due to RTR variability. Thus, the total standard deviation is

$$\sigma_{tot} = \sqrt{\sigma_{sys}^2 + \sigma_{RTR}^2} \qquad \text{(Eq. 3)}$$

Fig. 4b shows the effect of RTR variability on the fragility curves of degraded and non-degraded RC shear walls. The flatter curves are the result of the increase in the c.o.v. For this case, a flatter fragility curve increases the failure probability because the mean ultimate strength S_a is 4.14 g.

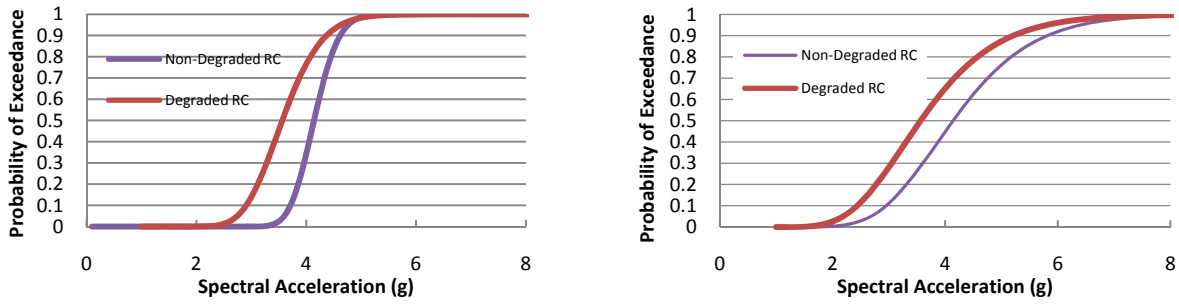

Fig. 4. Fragility Curve for the Base Shear at Ultimate Strength Limit State of the Shear Wall Model. (a) System Parameter Variability and (b) System Parameter and RTR Variability.

Hazard Curve for Seismic Evaluation

To model the effect of aging on the failure probability of structural systems, a hazard curve corresponding to a high seismic hazard zone was selected. The curve is based on the data provided by ASCE/SEI [7] for a site in California, USA, and a structure with a natural frequency of 10 Hz (i.e., fundamental period of vibration T = 0.1s.) This frequency is close to the frequency range of nuclear facilities in which lateral resistance is provided by shear walls and soil-structure interaction effects are limited. Fig. 5 shows the hazard curve points obtained from ASCE/SEI [7]. Approximated exponential and power-law relationships are also presented. In this example, the exponential curve (Eq. 4) is a better fit to compute the failure probability in this example than the power-law equation suggested by Jalayer [11] because the evaluated shear wall has a large ultimate strength.

$$\nu_{S_a(T)}(S_a) = P[S_a(T) \geq S_a] = k_o e^{-k.S_a} \quad \text{(Eq. 4)}$$

$\nu_{S_a(T)}(S_a)$ is the mean annual frequency of the ground motion having a spectral response acceleration at the system period larger than S_a. For very small probabilities, it is close to the annual probability of exceedance.

To obtain the probability of failure at the ultimate strength limit state, numerical integration was used to convolute the fragility curve of the shear wall at ultimate strength and the adopted hazard curve:

$$\lambda = \int_0^\infty F_C(x)\,|d\nu(x)| \quad \text{(Eq. 5)}$$

This equation expresses the probability of failure in terms of the fragility curve for a given median base shear strength over a S_a hazard curve pertaining to a specific site. If the only probabilistic parameters are the shear wall variables (i.e., capacity parameters), the failure probability for non-degraded system is $\lambda_{ND,\nu_{sys}} = 2.1 \times 10^{-8}$, whereas for degraded parameters the failure probability is $\lambda_{D,\nu_{sys}} = 2.4 \times 10^{-7}$. That is, the probability of failure increases more than one order of magnitude (11.4 times) due to aging degradation. However, when uncertainty due to RTR variability (i.e., demand parameters) was included in the calculations, the probability of failure of the non-degraded system increased to $\lambda_{ND,\nu_{tot}} = 2.8 \times 10^{-7}$, and when aging effects were included, the probability of failure was $\lambda_{D,\nu_{tot}} = 1.2 \times 10^{-6}$. The effect of RC degradation is not as pronounced when variability in the demands is included, and the probability of failure increases only four times due to aging effects.

This information is being used to model a generic two-story RC shear wall structure to verify some of the results obtained for the shear wall model. The main aging factors to be included will be (i) loss of steel area, (ii) changes in concrete compressive strength, and (iii) loss of concrete area due to cracking and spalling effects.

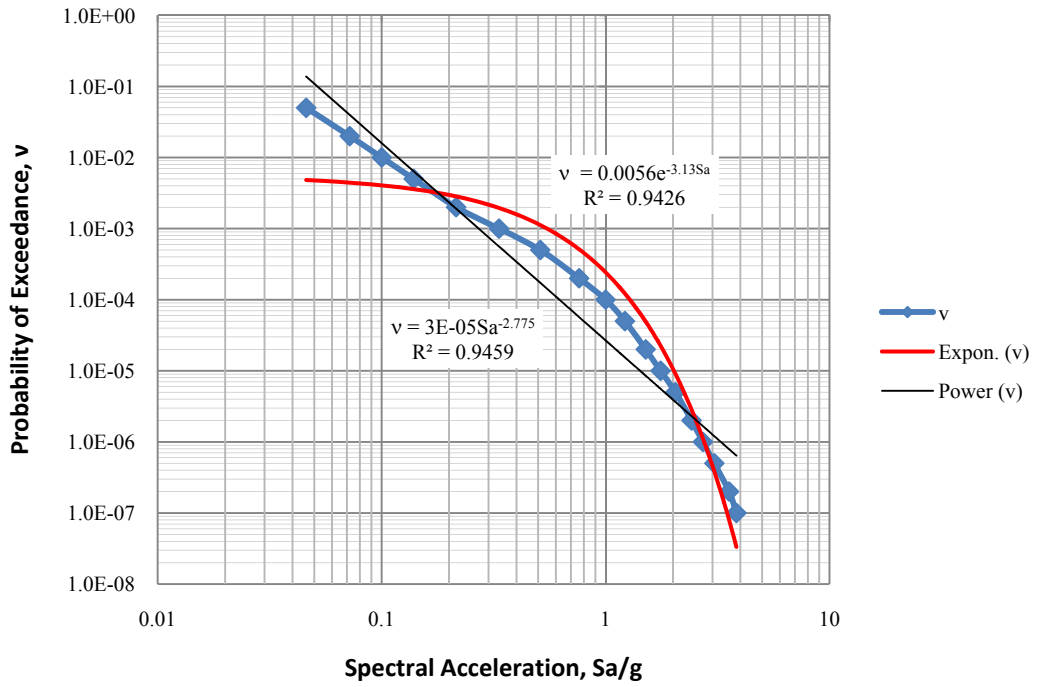

Fig. 5. Hazard Curve for Seismic Evaluation

CONCLUSIONS

The effect of aging of concrete on the seismic performance of reinforced concrete shear walls was evaluated in this study. The main findings are as follows:

- The increase on the concrete compressive strength with time does not overcome the degradation of seismic performance caused by concrete cracking and corrosion of steel rebars.
- Aging effects on reinforced concrete systems cannot be decoupled from the seismic hazard at the site.
- Aging effects increase the probability of failure of RC reinforced concrete shear walls subjected to lateral loading. Although a large reduction of steel area was considered (20%), RC degrading effects were not as pronounced when variability in the demand was included, and the probability of failure increased only four times due to aging effects.
- An exponential equation may be a better hazard curve approximation for cases in which the system capacity is rather high.

Aging of concrete may have different effects on the structure due to the system failure mechanism. Thus, it is recommended to perform similar studies on shear walls with larger aspect ratios that are more likely to develop bending failure. Also, the onset of non-linear behavior needs to be investigated in detail.

ACKNOWLEDGMENTS

This work was supported by Southwest Research Institute Internal Research and Development Project 20.R8090. The authors gratefully acknowledge the technical review of Dr. T. Wilt, the programmatic review of Dr. S. Mohanty, and the assistance of L. Gutierrez in the preparation of this manuscript.

REFERENCES

[1] Kennedy, R.P. and M.K. Ravindra. "Seismic Fragilities for Nuclear Power Plant Risk Studies." *Nuclear Engineering and Design*. Vol. 79. pp. 47–68. 1984.

[2] Braverman, J.I., C.A. Miller, B.R. Ellingwood, D.J. Naus, C.H. Hofmayer, S. Shteyngart, and P. Bezler. NUREG/CR–6715, "Probability-Based Evaluation of Degraded Reinforced Concrete Components in Nuclear Power Plants." Washington, DC: NRC. April 2001.

[3] Mori, Y. and B.R. Ellingwood. "Reliability-Based Service-Life Assessment of Aging Concrete Structures." *Journal of Structural Engineering*. Vol. 119, No. 5. pp. 1,600–1,621. 1993.

[4] Computers and Structures, Inc. "Structural Analysis Program." SAP2000, Vol. 14. Berkeley, California: Computer and Structures, Inc. 2009.

[5] Barda, F., J.M. Hanson, and W.G. Corley. "Shear Strength of Low-Rise Walls With Boundary Elements. Reinforced Concrete Structures in Seismic Zones SP–53." Detroit, Illinois: American Concrete Institute. pp. 149–202. 1977.

[6] Mander, J.B., M.J.N. Priestley and R. Park. "Theoretical Stress-Strain Model For Confined Concrete". Vol. 114 (8), pp. 1804-1826. 1988.

[7] American Society of Civil Engineers. "Seismic Design Criteria for Structures, Systems, and Components in Nuclear Facilities." ASCE/SEI 43–05. Reston, Virginia: American Society of Civil Engineers. 2005.

[8] Chiang, K., L. Ibarra, and B. Dasgupta. "Effect of Temperature on the Compressive Strength of Concrete." Transactions of SMiRT 21, Paper ID# 546. New Delhi, India. 2011. (Submitted)

[9] Wyss, G.D. and K.H. Jorgensen. "A User's Guide to LHS: Sandia's Latin Hypercube Sampling Software." SAND98–0210, UC–505. Albuquerque, New Mexico: Sandia National Laboratories. February 1998.

[10] Ibarra LF, and Krawinkler H (2005) "Global Collapse of Frame Structures Under Seismic Excitations." Pacific Earthquake Engineering Research (PEER) Report 2005/06, PEER Center, University of California, Berkeley, September 2005.

[11] Jalayer, F. "Direct Probabilistic Seismic Analysis: Implementing Non-Linear Dynamic Assessment". PhD. Dissertation, Department of Civil Engineering, Stanford University, California. 2003.